Scanning Laser Vibrometer Measurement of Guided Waves in Rails

Philip W. LOVEDAY, Craig S. LONG

CSIR Material Science and Manufacturing; Pretoria, South Africa
ploveday@csir.co.za , clong@csir.co.za

Abstract

Guided wave based inspection and monitoring systems for railway tracks operate at frequencies where as many as 40 modes of propagation may exist. During the development of such systems it is advantageous to be able to measure the amplitude of the individual modes of propagation. The availability of scanning laser vibrometer systems has made it possible to measure the displacement or velocity at a large number of points on the rail surface. The contribution of each mode of propagation may be estimated from the measured frequency responses by using a pseudo-inverse technique and mode shape information computed from a semi-analytical finite element model. Scanning laser measurements were performed in the field at distances of 10m and 500m from a transducer used to transmit the guided waves. A scan of 430 measurement points was used to measure 25 modes at 40kHz.

Keywords: Guided waves in rails, mode measurement, scanning laser vibrometer

1. Introduction

Railway tracks present an opportunity to exploit the advantages of guided wave ultrasound for NDT applications, as the rails are essentially one-dimensional waveguides allowing transmission over considerable distances from fixed transducer locations. To utilize this phenomenon it is often desirable to be able to measure the propagation in terms of individual modes of propagation or individual travelling waves. This situation occurs when one wishes to measure the attenuation of particular modes of propagation with distance or when developing a transducer to excite a particular mode of propagation. The measurement of reflection and transmission coefficients also requires measurement of individual modes of propagation.

This problem has been investigated by various authors and for various structures [1-5]. A similar problem is encountered when designing transducer arrays for transmitting or receiving specific guided waves [6]. If the mode shapes are known this information can be utilized in the extraction or separation process. In the case of pipes, the circumferential shape does not change with frequency, but in rails the mode shapes vary with frequency and need to be determined numerically. Mode shapes and dispersion relations obtained from a semi-analytical finite element (SAFE) analysis have been used in the mode extraction process [7]. The mode extraction theory is presented briefly in section 2. In [7] a few modes of propagation were extracted from measurements in the lab using tone-burst excitation. A relatively low frequency range was used where only eight modes are able to propagate and a set of 15 measurement points was arbitrarily selected. At higher frequencies, where between 20 and 40 modes propagate, the problem becomes more complicated.

The use of a scanning laser vibrometer makes it possible to measure responses at a large number of measurement points, limited only by accessibility. Some of the practical issues involved in performing scanning laser measurements in the field will be discussed in section 3. Field measurements and the application of the mode extraction process to these measurements are described in section 4.

2. Mode extraction theory

An intuitive explanation of how the mode shapes can be used to separate the propagating modes in cylinders is provided in [6] before the more general case is stated. The description presented here is similar to that in [7].

The frequency response of the waveguide, far from the excitation transducer and other irregularities can be written as a superposition of the propagating modes:

$$r(z,\omega) = \sum_{r}^{3N} \psi_{ir}(\omega)\alpha_r(\omega)e^{-j\kappa_r(\omega)z}, \tag{1}$$

where $\psi_{ir}(\omega)$ is the displacement of degree of freedom i of mode shape r and $\kappa_r(\omega)$ is the wavenumber of mode r. A SAFE analysis of the rail provides the term $\psi_{ir}(\omega)e^{-j\kappa_r(\omega)z}$. Field measurements may be performed at a singe frequency using a continuous sine wave excitation or simultaneously at a number of frequencies. We wish to extract the magnitude and phase of each propagating mode ($\alpha_r(\omega)$) from experimental time response measurements.

If we perform measurements at p different points each at a distance and location on the rail circumference and in a particular direction, the response can be written as a superposition of the contributions of the forward propagating modes, which can be written in the form $D(\omega)\alpha(\omega) = r(\omega)$ as:

$$\begin{bmatrix} \psi_{11}(\omega)e^{-j\kappa_1(\omega)z_1} & \psi_{12}(\omega)e^{-j\kappa_2(\omega)z_1} & \cdots & \psi_{1m}(\omega)e^{-j\kappa_m(\omega)z_1} \\ \vdots & \vdots & & \vdots \\ \psi_{p1}(\omega)e^{-j\kappa_1(\omega)z_p} & \psi_{p2}(\omega)e^{-j\kappa_2(\omega)z_p} & \cdots & \psi_{pm}(\omega)e^{-j\kappa_m(\omega)z_p} \end{bmatrix} \begin{Bmatrix} \alpha_1(\omega) \\ \alpha_2(\omega) \\ \vdots \\ \alpha_m(\omega) \end{Bmatrix} = \begin{Bmatrix} r_1(\omega) \\ \vdots \\ r_p(\omega) \end{Bmatrix}. \tag{2}$$

The mode shape matrix D is assembled from information from the SAFE model while vector r is assembled by performing a FFT on each of the measured time domain signals. Matrix D has dimension [p x m], while α is [m x 1] and r is [p x 1]. If p is equal to m (number of measurement points equal to number of modes) the matrix D is square and can be inverted. However, we expect a better result if we use additional measurement points ($p > m$) and solve the over-defined system of equations in a least-squares sense. This can be conveniently achieved by using the Moore-Penrose generalised inverse (also called the pseudo inverse). We expect that the matrix D will be rank m if there are at least m different propagating modes at the frequency of interest. The generalised inverse of D, in this case, is $D^{\dagger} = [D^*D]^{-1}D^*$, where D* is the Hermitian transpose of D and an estimate of α is obtained from $\tilde{\alpha} = D^{\dagger}r$. The condition number of the mode shape matrix was studied as a means for selecting a set of measurement locations [8].

If it is necessary to include both forward and backward propagating modes this can easily be done as the backward propagating modes are also provided by SAFE analysis. The system is then,

$$\begin{bmatrix} D_f(\omega) & D_b(\omega) \end{bmatrix} \begin{Bmatrix} \alpha_f(\omega) \\ \alpha_b(\omega) \end{Bmatrix} = r(\omega) \ . \tag{3}$$

The accuracy of the extraction process can be checked by computing the displacements at each scan point from the mode shape matrix and the extracted modal coefficients.

$$D(\omega)\tilde{\alpha}(\omega) = \tilde{r}(\omega) \tag{4}$$

In this way we can measure how well the extracted values fit the measured values and we can define an average mean squared error:

$$ERROR = \frac{1}{p}\left[\{r - \tilde{r}\}^* \cdot \{r - \tilde{r}\}\right]^{\frac{1}{2}} \tag{5}$$

3. Implementation in the field

Various issues need to be considered when performing measurements in the field. The selection of measurement points is determined by accessibility of the measurement points and the time available to perform scans. Measurements of the horizontal displacement on one side of the rail can be performed relatively easily as these measurements are not severely disrupted by passing trains. Measurements of vertical displacement on the crown and on the foot of the rail can be performed by positioning the scanning head above the rail. These scans can only be performed between trains. A study of the selection of measurement points [8] showed that the vertical measurements are very important for detecting most of the propagating modes and can be used alone without the horizontal measurements. The horizontal measurements are useful to supplement the vertical measurements but cannot be used without the vertical measurements. Considering that the rail boundary conditions change when a train passes, which may change the propagating modes it is necessary to perform the vertical and horizontal measurements between trains.

While it is not necessary to know the distance from the excitation transducer it is very important to know the relative position of each scan point. The scanning system used in this research did not have a geometry measurement unit so the positions of the measurement points had to be measured manually. This was achieved by measuring the physical position of three vertical measurement points on the rail and then calculating the position of the other points from the mirror angles of the scanning head while also taking into account the height difference between the head and the foot of the rail. The location of horizontal measurement points could be determined in a similar fashion with the requirement that the axial position relative to the vertical scan should be measured as carefully as possible.

The measurement points used do not coincide with node positions in the SAFE model, therefore the mode shapes were interpolated to provide displacements at the measurement points. The scan angles used were up to approximately 15° for a scan length of less than 1m. The scan angle could be taken into account by including axial displacement components of the mode shapes predicted by the SAFE model. An earlier investigation showed that the influence of this was negligible and this was not done in this study.

The excitation of the rail may be performed by various methods. In this work a small piezoelectric transducer was glued to the rail. It is essential that the excitation is repeatable and stable over the time of the scan. The positioning of the transducer influences the propagating modes that are excited. In addition, the scanning system requires a reference signal to synchronize the measurements. When the scan is performed close to the excitation

transducer it is possible to use the excitation signal as the reference signal. When large distances are involved it is possible to use a second piezoelectric transducer as a sensor to provide the reference signal. The excitation signal could be a tone burst as was used in the lab if the measurement distance is small or it can be a continuous signal such as random noise if many frequencies are to be measured simultaneously. If measurements at large distances are to be performed a better signal to noise ratio will be obtained by using a single frequency sine wave excitation and repeating the scan to measure other frequencies.

4. Field measurement results

Measurements were performed on Transnet's Coal Link line using a Polytec scanning laser vibrometer (PSV-400-M2-20) as shown in figure 1. The rail profile is S-60-SAR, which is similar to UIC60. Significant rail profile grinding has been performed over the years on this rail and the height of the rail was reduced by 14mm in the SAFE model to account for this. The dispersion curves, of propagating modes, computed from a SAFE model are shown in figure 2. The high density of propagating modes in the frequency range 30 to 50 kHz is illustrated.
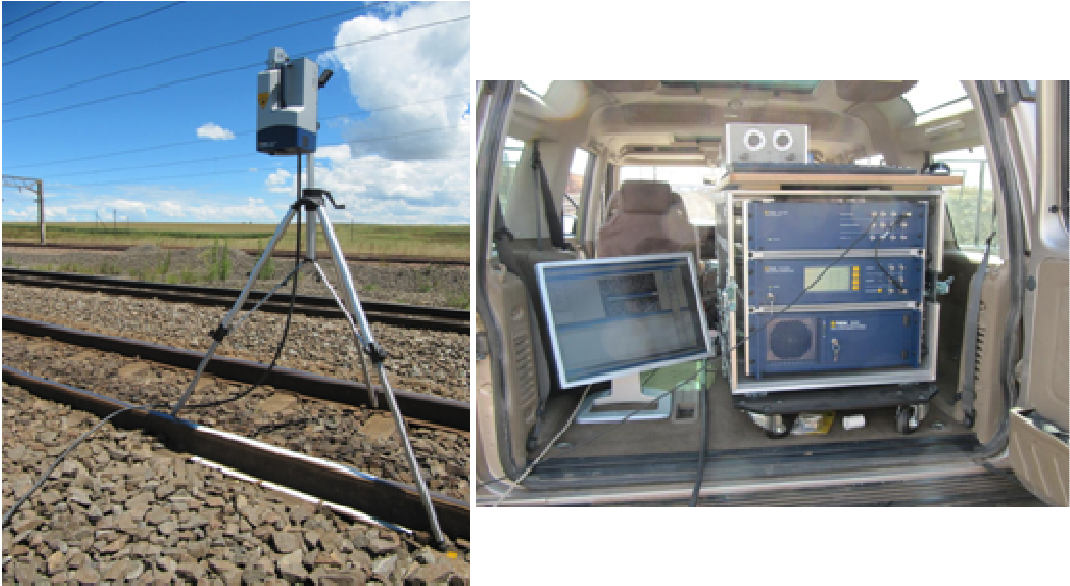

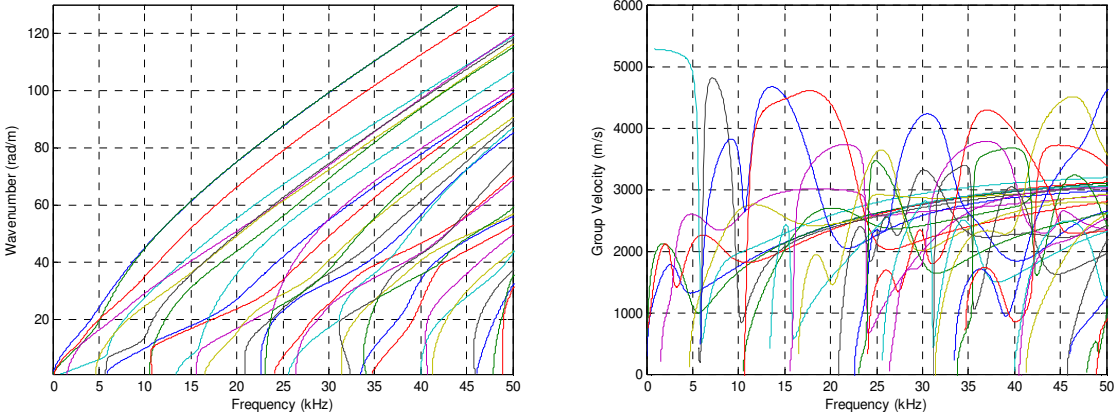Figure 1. Positioning of sensor head above rail

Figure 2. Computed dispersion curves

Only the vertical displacements were measured over a range of points. It is possible to measure horizontal displacements on one side of the rail and to include these in the mode measurement procedure. This does require that the positioning of the horizontal points relative to the vertical points is accurately known. Figure 3 shows a scan performed close (10m) to the excitation transducer and a scan performed at a distance of 500m from a different excitation transducer. In the first scan the function generator of the Polytec scanning system produced a 1 Vpk, 40 kHz sine signal, which was amplified to 20Vpk to drive the transmit piezoelectric transducer. The 1 Vpk signal was used as the reference signal for the scanning system. In the second scan a separate function generator was used at the transmit station (amplified to 80Vpk) and no connection to the scanning system was possible because of the distance involved. Instead, a second piezoelectric transducer was bonded to the rail and the signal detected by this transducer was used as the reference signal by the scanning system. It is essential to have a reference signal so that the relative phase of the measurements at each point can be measured.
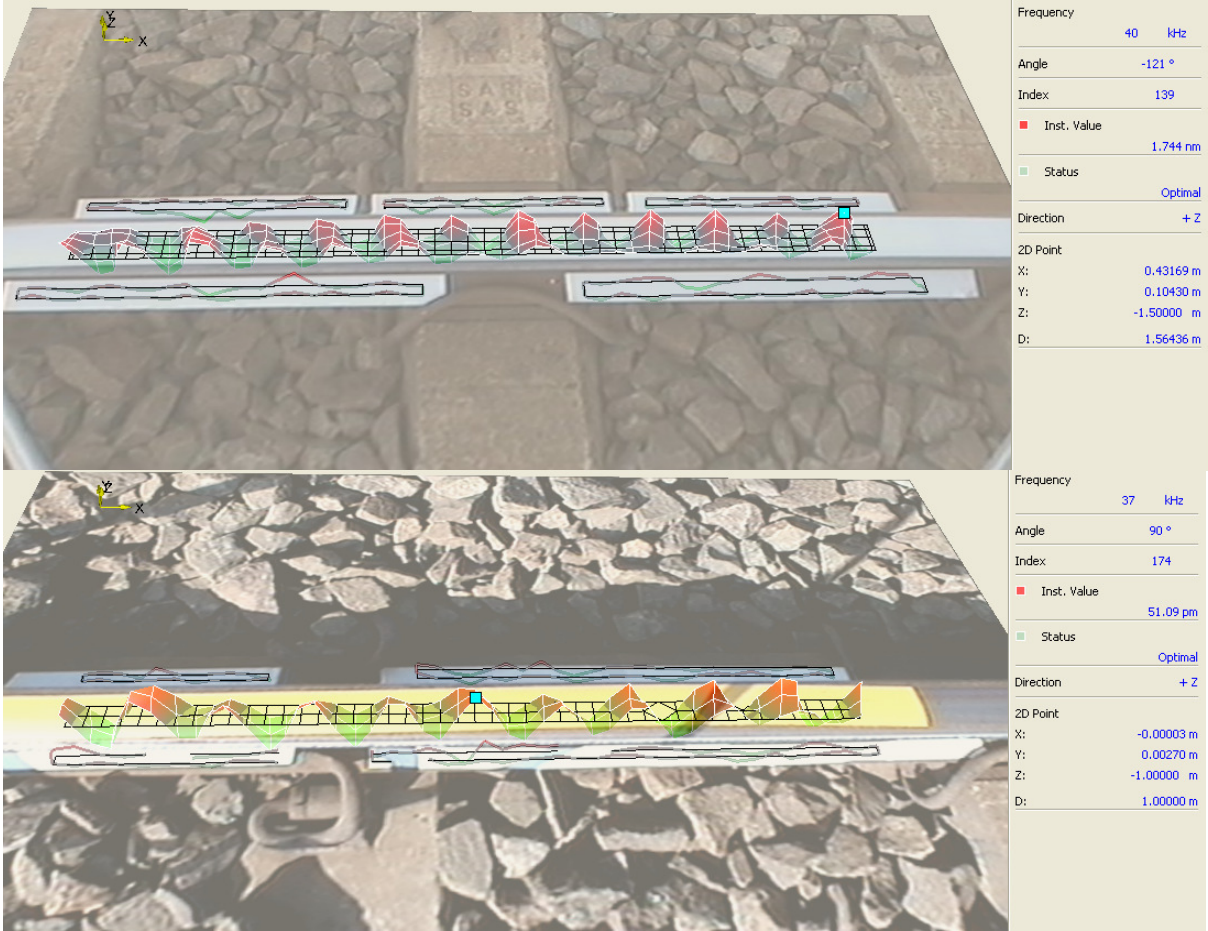

Figure 3. Typical scan results at 10m and 40kHz (top) and 500m and 37 kHz (bottom)

The mode extraction procedure described in section 3 was applied to the 40kHz scan, which has 430 measurement points. Once the modes are extracted the displacement at each point can be calculated and the error between the actual measured value and the fitted value determined. As the elastic modulus of the rail at 40 kHz was not known a range of modulii was used and the best fit was found. The error, computed by (5), is shown as a function of elastic modulus in figure 4 where it is seen that a modulus of 215 GPa produced the best fit. The measured and fitted displacement amplitude at each measurement point is shown in figure 5. The points have been ordered in the direction across the rail so the points on one foot are plotted first followed by the points on the head and then the points on the other foot.

It is evident that the elastic modulus of 215 GPa produced the best fit especially on the head of the rail.
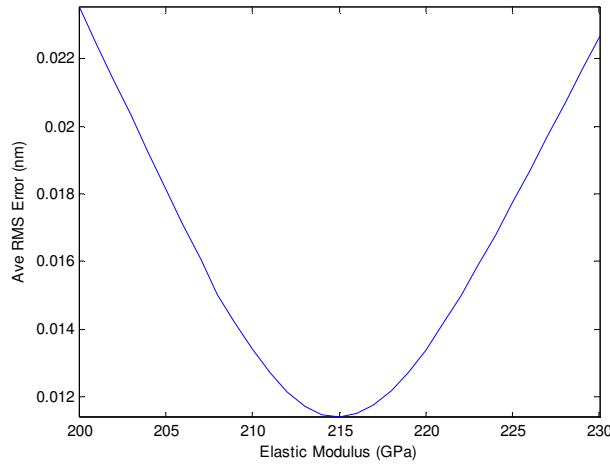

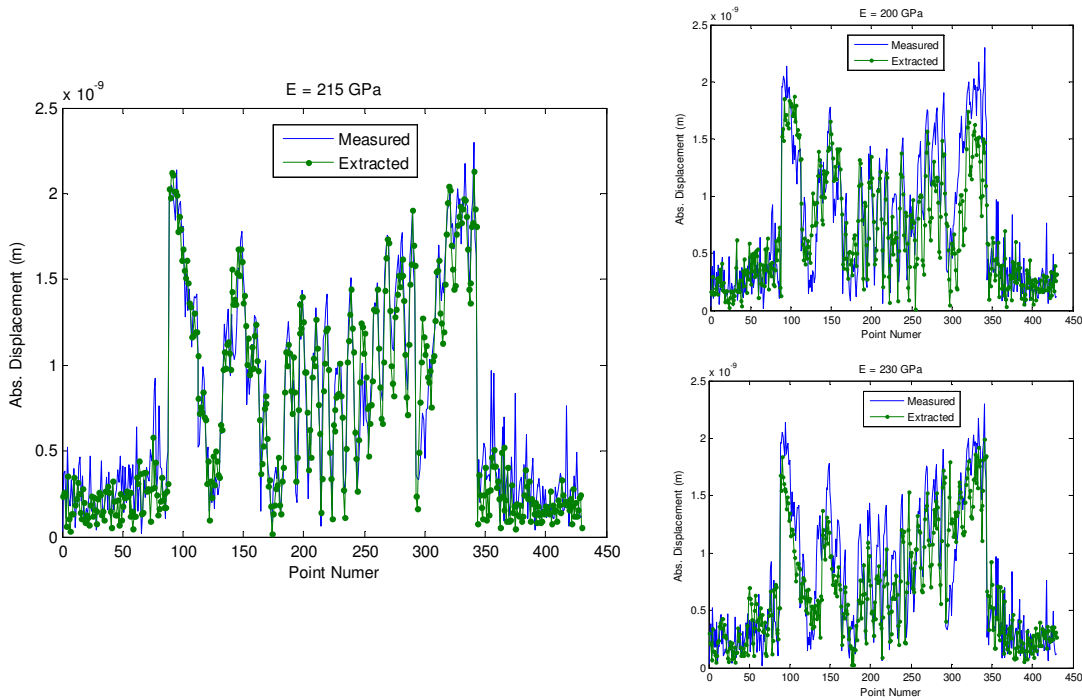Figure 4. Determining the elastic modulus that produces the lowest error

Figure 5. Measured and fitted displacement amplitudes for different elastic modulii

The amplitudes of the modal coefficients extracted by the process ($|\alpha_f|$, $|\alpha_b|$) are listed in table 1. The mode shapes were scaled to have unity maximum value. The table shows the wavenumbers for the 25 propagating modes at 40 kHz. Selected mode shapes are shown in figure 6 for purposes of discussion.

Table 1 shows that the extraction process reveals that modes 19, 21 and 22 are dominant and that the forward travelling wave is large compared to the backward travelling wave. These modes all have significant vertical motion of the head, which is expected. The extraction process indicated some response of modes 15 and 23. In particular the backward propagating mode 23 was larger than the forward travelling mode, which would not be expected. The mode shapes of these two modes reveal that there is very little vertical motion in these modes at our measurement points. This would make it difficult to measure these modes using only

the vertical measurement points. In addition, the extracted amplitudes would have small influence on the fitted curves as these modes contribute an insignificant amount. This is illustrated by removing these two modes from the extraction process. This is equivalent to setting the amplitude of these modes to zero. It was seen that this had negligible influence on the amplitude of the other extracted modes. The error in the curve fit was also unaffected.

The amplitudes of the extracted modes appears to be realistic as they are smaller than the maximum measured displacement amplitudes. Previous experience with insufficient or poorly selected measurement points produced large extracted modal amplitudes that fitted well (due to mode cancellation) over the measurement region but would predict very large amplitudes outside the measurement region. Extrapolation to other distances with the modal coefficients in table 1 would not result in unrealistically large amplitudes.

Table 1. Extracted mode amplitudes

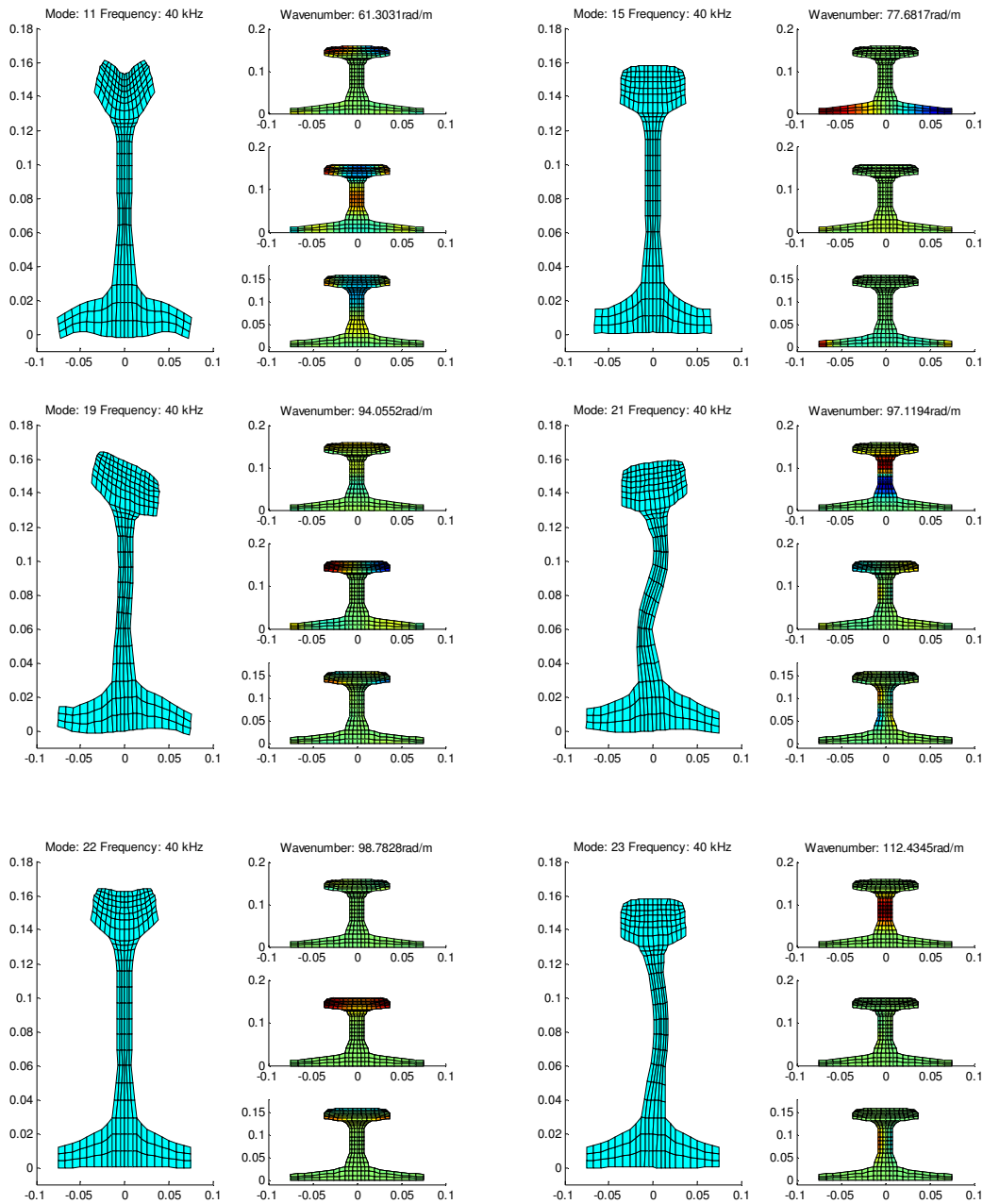| Mode No.	Wavenumber (rad/m)	Forward Amplitude (nm)	Backward Amplitude (nm)	Forward Amplitude (Mode 15 & 23 excluded) (nm)	Backward Amplitude (Mode 15 & 23 excluded) (nm)
1	2.07	0.05	0.01	0.05	0.01
2	25.72	0.03	0.02	0.02	0.03
3	33.99	0.11	0.06	0.11	0.07
4	35.71	0.52	0.31	0.51	0.31
5	40.51	0.19	0.39	0.19	0.39
6	42.79	0.25	0.18	0.25	0.19
7	43.18	0.50	0.48	0.50	0.48
8	46.60	0.28	0.45	0.29	0.44
9	54.84	0.05	0.08	0.05	0.08
10	56.53	0.25	0.11	0.25	0.11
11	61.30	0.95	0.04	0.95	0.04
12	67.60	0.28	0.01	0.28	0.01
13	70.83	0.36	0.14	0.33	0.14
14	75.33	0.06	0.07	0.08	0.07
15	77.68	0.21	0.19	-	-
16	79.66	0.23	0.12	0.23	0.13
17	85.85	0.36	0.07	0.35	0.07
18	93.76	0.64	0.04	0.64	0.04
19	94.06	2.15	0.17	2.15	0.18
20	96.75	0.06	0.03	0.06	0.03
21	97.12	1.58	0.30	1.60	0.30
22	98.78	1.83	0.08	1.83	0.08
23	112.43	0.24	0.80	-	-
24	121.08	0.14	0.03	0.14	0.03
25	121.09	0.15	0.12	0.15	0.12

Figure 6. Selected mode shapes at 40 kHz computed by SAFE. Contour plots show horizontal (top), vertical (middle) and axial (bottom) displacements respectively.

5. Conclusions

A technique for measuring the individual modes of propagation in rails from scanning laser vibrometer measurements was presented. Measurements were performed in the field, which demonstrated the capability of performing scans even when the propagating modes are small at a distance of 500m from the excitation. The extraction process was applied to extract 25 modes at 40 kHz and appears to accurately measure the individual modes of propagation.

Acknowledgements

References

1. D. Alleyne and P. Cawley, 'A two-dimensional Fourier transform method for the measurement of propagating multimode signals', J. Acoust. Soc. Am*., Vol. 89, pp 1159-1168, 1991.
2. D. J. Thompson, 'Experimental analysis of wave propagation in railway tracks', J. Sound Vib*., Vol. 203, No. 5, pp 867-888, 1997.
3. D. Gsell, D. Profunser and J. Dual, 'Measurement of the dispersion relation of guided non-axisymmetric waves in filament-wound cylindrical structures', Ultrasonics*, Vol. 38, pp 517-521, 2000.
4. F. Lanza di Scalea and J. McNamara, 'Measuring high-frequency wave propagation in railroad tracks by joint time-frequency analysis', J. Sound Vib*., Vol. 273, pp 637-651, 2004.
5. T. Hayashi and M. Murase, 'Mode extraction technique for guided waves in a pipe', NDT and E., Vol. 20, No. 1, pp 63-75, 2005.
6. P. D. Wilcox, 'Guided-Wave Array Methods' in Encyclopedia of Structural Health Monitoring, 2009.
7. P.W. Loveday, 'Measurement of Modal Amplitudes of Guided Waves in Rails', Proc. of SPIE, Vol. 6935, 2008.
8. P.W. Loveday and C.S. Long, 'Modal amplitude extraction of guided waves in rails using scanning laser vibrometer measurements', to appear in Rev. Prog. QNDE, 2011.